Hindawi
Mathematical Problems in Engineering
Volume 2023, Article ID 1384964, 10 pages
https://doi.org/10.1155/2023/1384964

Research Article

Deformation Characteristics and Control Mechanisms of Deep High-Stress Large-Span Roadways

Bo Yang [1,2] **and Jing Chai** [1,3]

[1]*Xi'an University of Science and Technology, Xi'an, Shaanxi 710000, China*
[2]*Shanxi Institute of Energy, Jinzhong, Shanxi 030600, China*
[3]*Key Laboratory of Western Mine Exploitation and Hazard Prevention, Xi'an University of Science and Technology, Ministry of Education, Xi'an, Shaanxi 710000, China*

Correspondence should be addressed to Jing Chai; chaij@xust.edu.cn

Received 15 September 2022; Revised 30 October 2022; Accepted 24 November 2022; Published 2 February 2023

Academic Editor: Fuqiang Ren

Controlling the surrounding rock in soft rock roadways under deep high stress, strong rheology, and intensive mining is critical for the safety, efficiency, and economy of mine production. In this study, the mechanical properties, large deformation mechanism, and support countermeasures of surrounding rock in the high-stress roadway in the Yuwu coal mine were systematically explored through laboratory tests, numerical calculations, and field measurements. It is shown that mudstone and sandstone are mainly composed of chlorite and kaolinite, respectively. Also, mudstone features elastoplasticity and experiences argillization and swelling in water. The mechanism of surrounding rock deformation in the high-stress roadway in the Yuwu coal mine was determined. As the V-shaped shear zone in the side corner expanded to the deep under high deviatoric stress, large-scale tensile damage occurred in the shallow surrounding rock. Consequently, discontinuous stresses in deep and shallow parts induce the expansion and fracturing of the roadway. The deformation velocity and damage degree of surrounding rock rise exponentially under different stress release coefficients, so the reduced distance of the face roof under control and timely support is important for restricting the free surface. An idea of "timely and active reinforcing the side and strengthening the bottom" was proposed. This approach made the loads on all the support objects within the working range. The overall deformation of the surrounding rock was controlled within 350 mm, ensuring the long-term stability of the roadway.

1. Introduction

Due to its mechanical properties and complex stress fields, deep roadway surrounding rock features significant strength attenuation and fast deformation [1–6]. Under the superimposed effect of high stress and strong mining, surrounding rock experiences continuous and discontinuous deformation and even disasters [7]. Therefore, clarifying the microscopic characteristics and macromechanical properties of deep surrounding rock and the stress release characteristics of deep roadways is crucial for developing deep roadway control technology.

In order to increase the stability of surrounding rock in deep roadways, researchers have carried out extensive work in terms of the type, mechanism, and control technology of surrounding rock deformation. The deformation of roadway surrounding rock is mainly induced by the nature of rock strata (e.g., the significant strength attenuation due to argillization in water), stress (the postpeak rock dilation, integrity reduction, and strength attenuation caused by the joint effects of pure shear, bending and tensile shear), and structure (e.g., special geological tectonic zones) [8, 9]. Based on numerical calculations, Liu and Sun [10] proposed that the failure mode of deep roadway surrounding rock changes from tensile failure to shear failure with increased depth. Wang et al. [11] suggested a method for the support of roadways in deep mining areas with high-strength bolt-grouting. Based on a self-developed deep-ground testing

device, Xu et al. [12] generalized the whole process of roadway instability using various monitoring methods and concluded that the surrounding rock instability is induced by discontinuous stresses (as a result of internal stress drop) in the shallow and deep. Li et al. and Wang et al. [13, 14] identified the zonal fracturing characteristics of deep surrounding rock and developed a constitutive applicability model. Deep roadway control mainly enhances the coupling strength and enlarges the angle of high-stress coordinated deformation of surrounding rock. The main methods include passive support, active support, repair and reinforcement, pressure release and transfer, and the joint method [15, 16]. Different types of surrounding rock should be reinforced by different methods. Based on the reserved deformation, Yu et al. [17] proposed a comprehensive support and repair strategy using a bolt, metal mesh, shotcrete, grouting, anchor cable, and combined anchor cable. Considering the boundary shape characteristics of the plastic zone, Guo et al. [18] reported the evaluation criterion of the location of potential hazards and critical evaluation points of dynamic roadway disasters. Yang et al. [19] considered that the shallow tensile fracturing and large expansion are the root causes of roadway floor heave and roof cut-off and presented a new joint support method of "anchor bolt-anchor cable-metal mesh-sprayed concrete and shell." Concerning the asymmetric stress and damage zone of roadways, Zhu et al. [20] introduced the "three shells" collaborative support technology for large-section chambers in deep mines. Li et al. [21] explored the influence of anchoring agent with high sand content, mechanical anchoring means, or grouting reinforcement on the anchoring force.

The failure mechanism of surrounding rocks in deep roadways has always attracted much attention. Zhao et al. [22] considered that the maximum and minimum stresses deteriorated gradually with the increase of time after roadway excavation, and the failure zones in soft rock mass expanded increasingly over time. Zhan et al. [23] analyzed the stability control theory of soft-rock roadways based on the Nishihara model and Drucker–Prague's modification of the Mohr–Coulomb yield condition. Jia et al. [24] proposed the nonlinear creep constitutive model of soft rock and its numerical realization method by the indoor creep test of soft rock and the large-scale triaxial creep tests on-site. Zhan et al. [25] reported that combining the parts organically and coordinating their bearing performance effectively realize the stability control of large nonlinear deformation. Zhu et al. [26] divided the surrounding rock stress and roadway deformation characteristics into advance influence, rapid change, and stability stages. The new support technologies for deep soft rock roadways were put forward based on mechanism research. Li et al. [1] proposed a "double layer bolt-mesh-shotcrete and U-shaped steel" supporting scheme by numerical simulations and field tests, effectively solving the problem of large deformation and failure of deep soft rock roadway. Yuan et al. [27] introduced a method of bolt-net-cable-grout coupling support and achieved good results in practical application, effectively solving the support issues of high-stress broken soft rock roadway in deep mines. Yang et al. [28] explored a new, improved method of support called the "bolt-cable-mesh and shell" support scheme, which could change the stress state of surrounding rock especially roadway floor. Zhao et al. [29] proposed "shotcreting, grouting anchor bolt, anchor bolt, grouting anchor cable, and anchor cable" compound timbering fashion. The rationality of the supporting technology was corroborated by theoretical analysis, engineering analogy, engineering practice, and numerical simulations.

The above studies have enriched the theory and practice concerning stability control of deep roadway surrounding rocks [30, 31]. However, these analyses were made from a macroscopic perspective, neglecting the stress release characteristics of surrounding rock corresponding to the actual roadway support timing. Therefore, considering the large buried deep roadways in the Yuwu coal mine as the case study, the microstructure, macromechanical properties, grade classification, and damage characteristics of surrounding rock under different stress release coefficients were analyzed in this paper. On this basis, a surrounding rock reinforcement method was proposed to provide a reference for supporting deep roadways in similar geological conditions.

2. Occurrence Conditions and Macro and Microcharacteristics of Roadway Surrounding Rock

2.1. Occurrence Conditions of Roadway Surrounding Rock. The Yuwu coal mine is located southeast of Shanxi province, west of the Lu'an mine area. Its longitude and latitude range is 112°47′–112°54′ east and 36°15′–36°25′ north (Figure 1). The mine has its railroad line linked to the Chinese railroad system, which can realize the transportation of coal nationwide, and the transportation is very convenient. The geographical location map involves copyright and issues related to confidentiality. On average, the No. 3 coal seam of the Yuwu coal mine is 6.4 m thick. Along the floor of the S5203 transportation roadway, its main roof, immediate roof, and immediate floor are medium sandstone, sandy mudstone, and mudstone, with average thicknesses of 18 m, 1.3 m, and 3.2 m, respectively. The roadway, whose size is 5,400 mm × 3,800 mm, presents the phenomenon of roof water trickling in its partial area. The maximum principal stress is in the vertical direction of the mine, i.e., the vertical stress is the maximum stress, and the horizontal stress is 0.5–1.0 times as high as the vertical stress. The principal and horizontal stresses of the S5203 transportation roadway are 14.3 MPa and 13.1 MPa, respectively.

2.2. Macro and Microcharacteristics of the Surrounding Rock. Samples were taken from the roof and floor of the S5203 roadway on-site and processed into a standard cylinder size (50 mm diameter × 100 mm height) in the laboratory for a uniaxial compression test. Also, rock powders with different lithologies were processed for X-ray diffraction tests to analyze their mineral compositions. The specific test results are shown in Figure 2. Mudstone has a long compression phase, strong postpeak plasticity, a small elastic modulus

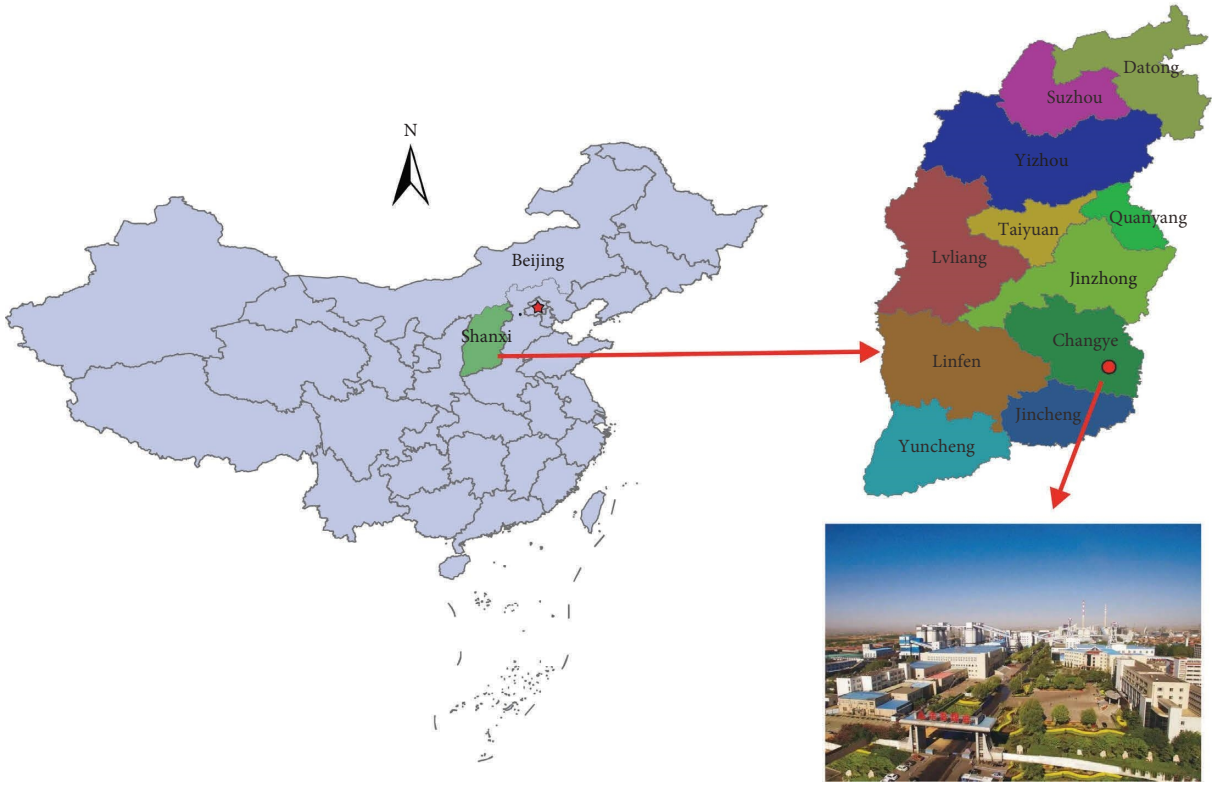

Figure 1: Geographic location and mining map of the Yuwu coal mine.

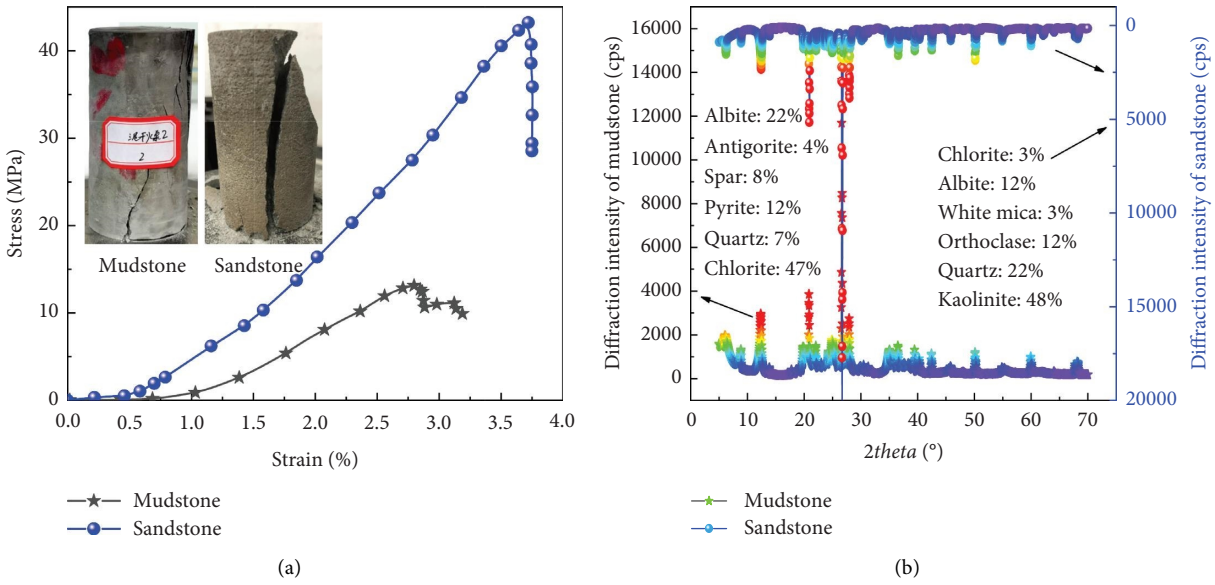

Figure 2: Macro and microcharacteristics of rocks of different lithologies: (a) stress-strain curves and (b) mineral compositions.

(0.8 GPa), and a low peak strength (13.1 MPa). Sandstone exhibits a high fracturing strength and a remarkable elastic brittleness, with an elastic modulus and a peak strength of 2.0 GPa and 43.2 MPa, respectively. It can be seen from the mineralogical compositions of mudstone and sandstone that mudstone is mainly comprised of sodium feldspar (22%) and chlorite (47%). Chlorite has a flaky microstructure, and these flakes rub strongly with each other when damage occurs. However, chlorite softens while encountering water, inducing severe deformation of the roof and floor. Sandstone mainly comprises kaolinite (48%) and quartz (22%), with closely packed microscopic particles. This type of rock fractures severely when it fails, which is consistent with the laboratory observation of rock compression and fracturing.

2.3. Grade of Roadway Surrounding Rock. From the mechanical properties of the roof and floor of roadways, the level of ground stress, and the "Engineering Rock Classification Standard," it can be determined that the roof of roadways belongs to the high-stress area [32]. The floor and the two sides belong to the extremely high-stress area. The strength-to-stress ratio can be expressed as follows:

$$S_r = \frac{k_v R_c}{\sigma_{\max}}, \quad (1)$$

where k_v is the integrity factor, taken as 0.3–0.5 in this paper; $\sigma_{\max}$ is the maximum principal stress perpendicular to the direction of the roadway axis, MPa; R_c is the uniaxial compressive strength of the rock, MPa. Hence, the surrounding rock on the two sides and floor can be classified as Grade V, which is Grade II on the roof.

3. Stress Release and Deformation Characteristics of Surrounding Rock in a Deep Roadway

3.1. Model Validation and Large-Scale Modeling. In this paper, the deformation and damage characteristics of roadway surrounding rock were analyzed by the block distinct universal element code-grain boundary model (UDEC-GBM) [33, 34], as shown in Figure 3. The mechanical behavior of blocks is controlled by the mechanical properties of the crystal interface and the geometric features of the polygon. Once it exceeds the shear or tensile strength, the bond between particles breaks, producing compressive shear fractures, tensile fractures, or sliding fractures. Therefore, it can be considered an effective tool for studying the generation, initiation, and extension of fractures.

A uniaxial compression numerical model of the same size as the laboratory model was developed (including two steel plates on the roof and floor of the sample). The model employed inhomogeneous particle size distribution and a proven reasonable block length (3 mm). The upper and lower steel plates were applied with a constant velocity of 0.01 m/s in the Y-direction to guarantee a quasistatic state of the sample. The total reactive forces (which are continuously recorded) at the contact between the sample and the roof loading plate were the axial stresses.

The stress-strain responses of the sample exhibit an initial linear elastic trend without a compression phase. This is due to the disparity between the numerical calculations and laboratory results. The yielding phase was not noticeable. The sample mainly experienced axial splitting and tensile fracturing, consequently bearing macroscopic fractures parallel to the loading direction. Thus, tensile fractures were generated at the low-loading stress stage, and the shear fractures were generated at an accelerating rate during the yielding phase. Moreover, the shear fracture generation stage lasted longer, indicating that mudstone is strongly plastic.

Meanwhile, the rock compression process witnessed a shear localization effect and mixed damage of the axial splitting/shear zone, which belongs to the final phase. Sandstone had 1.3 times as many tensile fractures as mudstone. Nevertheless, the two types of rock were close in the number of shear fractures, indicating that postpeak tensile fracturing can indirectly characterize the elastic brittleness of the sample. The numerical calculation and laboratory test results can confirm the reasonableness of the simulation parameters and methods, which can be used to analyze the scenarios of large-scale roadway fracturing.

The large-scale numerical calculation model was close to the actual geological conditions (58 m length × 38 m height). The upper boundary of the model was stress constraint, which could characterize the overlying stratum load (14 MPa), and the left, right, and lower boundaries of the model were roller supports. The numerical model, local detail image of the roadway location, and numerical calculation model are shown in Figure 4 and Table 1.

3.2. Damage Characteristics of Deep Roadway Surrounding Rock

3.2.1. Deformation and Principal Stress Evolution Characteristics of a Roadway. The monitoring curves of displacements of the roof, floor, and the two sides at different stress release coefficients after mining are shown in Figure 5. The overall deformation of the roadway develops in a stepwise manner with a decrease in the stress release coefficient. The roadway deforms unevenly under unsupported conditions, with serious roof subsidence, floor heave, and side shrinkage occurring simultaneously. The left roof subsidies for about 520 mm. The heave of the right floor is slightly larger than that of the left floor; however, both are no larger than 530 mm. The left and right sides deform for 630 mm and 930 mm, respectively. In addition, the side deformation and floor heave are consistent.

It can be seen from the principal stress evolution under different stress release effects (Figure 6) that the stress is concentrated on the roadway surface, especially on the side corners where the stress is intensively concentrated. When the deflective stress reaches the shear strength, the surrounding rock becomes damaged, and the bearing capacity of the shallow surrounding rock is reduced. As the tensile stress zone continues to expand deeper, a large stress relaxation zone around the roadway is consequently formed. Hence, roadway support should be timely provided because a large stress release coefficient (little energy release) can effectively mitigate the overall displacement of the roadway and the magnitude of the stress environment. Given the synergistic deformation of the two sides, roof, and floor, the sides and floor should be supported synergistically; otherwise, the enlarged displacement of the sides will lead to stress transfer to the floor, thus inducing floor heave.

3.2.2. Damage and Fracturing Evolution of Surrounding Rock. Since the instability of underground engineering surrounding rock is closely related to the stress environment, plastic zone, and extension of fractures [18], it is of great significance to clarify the generation and extension of fractures in surrounding rock after mining in deep roadways. Blue and red lines mark unit and joint shear and

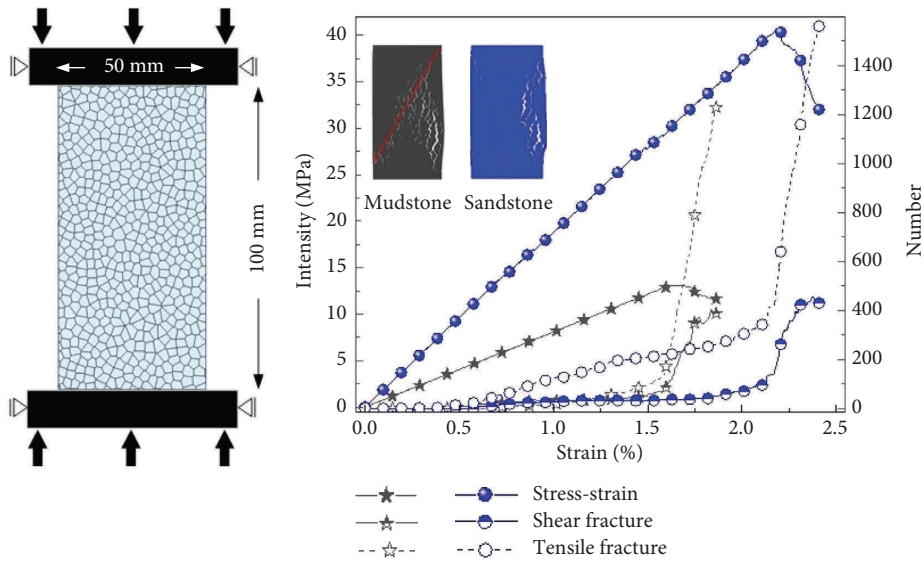

Figure 3: Numerical calculation model and model validation.

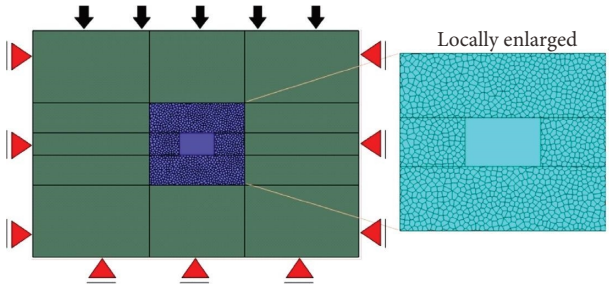

Figure 4: Numerical calculation model of severe deformation in a deep high-stress roadway.

Table 1: Numerical calculation parameters of severe deformation in a deep high-stress roadway.

Lithology	Block		Block/contact		Contact
	Elasticity modulus (GPa)	Cohesive force (MPa)	Internal friction angle (°)	Tensile strength (MPa)	Normal/tangential stiffness (GPa)
Mudstone	0.8	1.2/3.8	24/30	0.8/1.5	90/70
Sandstone	2.0	4/10	38/40	1.2/2.8	160/100
Coal seam	0.6	1.1/3.2	21/28	1.1/1.4	80/48

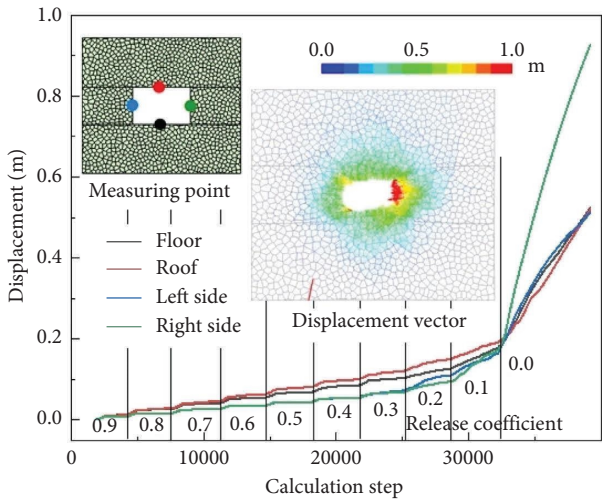

Figure 5: Monitoring of surrounding rock deformation at measuring points.

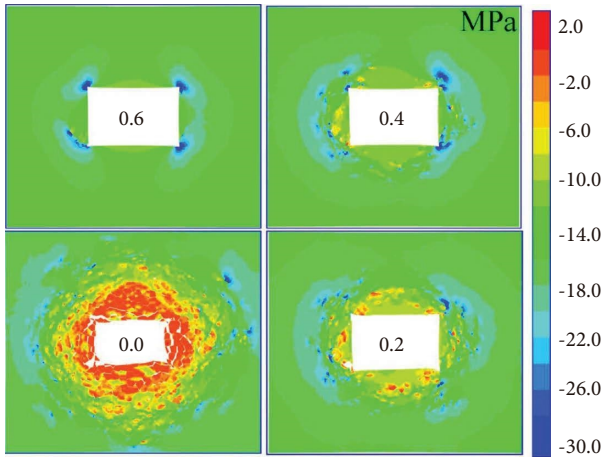

Figure 6: Evolution characteristics of principal stress.

tensile damages. Shear fractures that first appear in the side corners may cause shear extrusion damage, which is consistent with the principal stress distribution given in the previous study. As the V-shaped shear damage zone gradually deepens, the stress it releases will give rise to damage on the roof and floor, leaving a huge shear fracture zone in the deep and a tensile damage zone around the roadway surface. Compared with Figure 7, it is apparent that the tensile damage zone is exactly the area where surrounding rock displacement is large (Figure 5), as the tensile damage induces the fragmentation, expansion, and separation of surrounding rock. Since the surrounding rock is severely fragmented, the rock masses almost no longer rub or embed each other.

The unit damage evolution resembles the joint damage evolution, both surging at the stress release coefficient of 0.4. At a 0–30% relaxation state, the internal support pressure of the surrounding rock is sufficient to withstand spalling damage. However, the back-support pressure plummets at a 60% relaxation state, accompanied by a significant plasticity index. Spalling and roof-falling accidents are likely to occur near the roadway. Thus, it is critical to choose appropriate support measures and installation timings for the safety of workers and equipment. Installation timing is an important aspect of roadway reinforcement/support design. If the system is installed too early, the inducing roadway load may exceed the bearing capacity of the structural units. If too late, rock masses may already be irreversibly damaged and slackened.

3.3. Deformation Mechanism of Roadway in Yuwu Coal Mine. From the analysis presented previously, the deformation characteristics and mechanism of high-stress roadways in the Yuwu coal mine can be described as follows.

(1) Contradiction between high-ground stress and low-strength rock: The ground stress is high, while the surrounding rock is loose and soft. The mining-induced stress relief on the free side increases deflective stress, and hence, the high stress damages shallow surrounding rock around the roadway. As fractures expand from the middle of the roadway to the interior and surface, shallow surrounding rock loses its bearing capacity. In addition, the floor containing a large number of clay minerals will aggravate the deformation and damage when contacted with mine water during the mining process.

(2) Poor stress state around the roadway: Due to the poor stress state of the right angle, the high stress tends to be concentrated in the side corners. After the formation of a shear zone, the shallow part of the roadway becomes a free rock layer, which indirectly increases the span of the roadway and leads to a bending of the floor. Floor damage is inconducive to roadway stability because it causes roadway contraction and exacerbates roof subsidence. This vicious cycle will eventually result in the occupation of free space on the roadway.

4. Deep Surrounding Rock Control Technology

4.1. Support Idea and Scheme. From the results presented previously and the deformation characteristics and mechanism of deep surrounding rock in the Yuwu coal mine, the deep surrounding rock should be reinforced by timely and coordinated support to the roof, floor, and sides. The joint active support of anchor bolts (cables) and double steel joists is adopted in the roadway to improve the coupling performance of deep and shallow surrounding rock. Besides, passive support is adopted to control the initial and surface deformation of surrounding rock, i.e., I-shaped steel sheds are installed on the heading face.

For the roof, it is supported by yielding bolts with an interrow spacing of 830 mm × 700 mm and anchor bolts (cables) with an interrow spacing of 1,660 mm × 700 mm (in a 3-2-3 layout). The lengths of the bolt and cable are 2,400 mm and 6,300 mm, respectively. The two sides and the roof are equipped with metal meshes and double steel ladders. The specific parameters are given in Figure 8.

4.2. Effectiveness of Roadway Surrounding Rock Control. In order to verify the reasonableness of the support parameters proposed above, grasp the characteristics of surrounding rock deformation of deep surrounding rock roadways in the Yuwu coal mine, and test the effect of surrounding rock control, on-site monitoring was conducted on the S5203 roadway by taking surface displacement (at cross measuring points), anchor bolt stress, and anchor cable stress as indicators. The monitoring started at 5 m from the heading face.

Surface displacements of the roadway at different times are shown in Figure 9. The roof-to-floor and side-to-side convergences were 210 mm and 140 mm, respectively. Overall, the roadway just deformed mildly, and roof subsidence was slightly larger than the floor heave. The deformation of the two sides and the roof and floor stabilized on the 10th and 15th days, respectively. Meanwhile, during excavation, a thin sandy mudstone stratum was found in the immediate roof. On the 6th day, small fractures began to

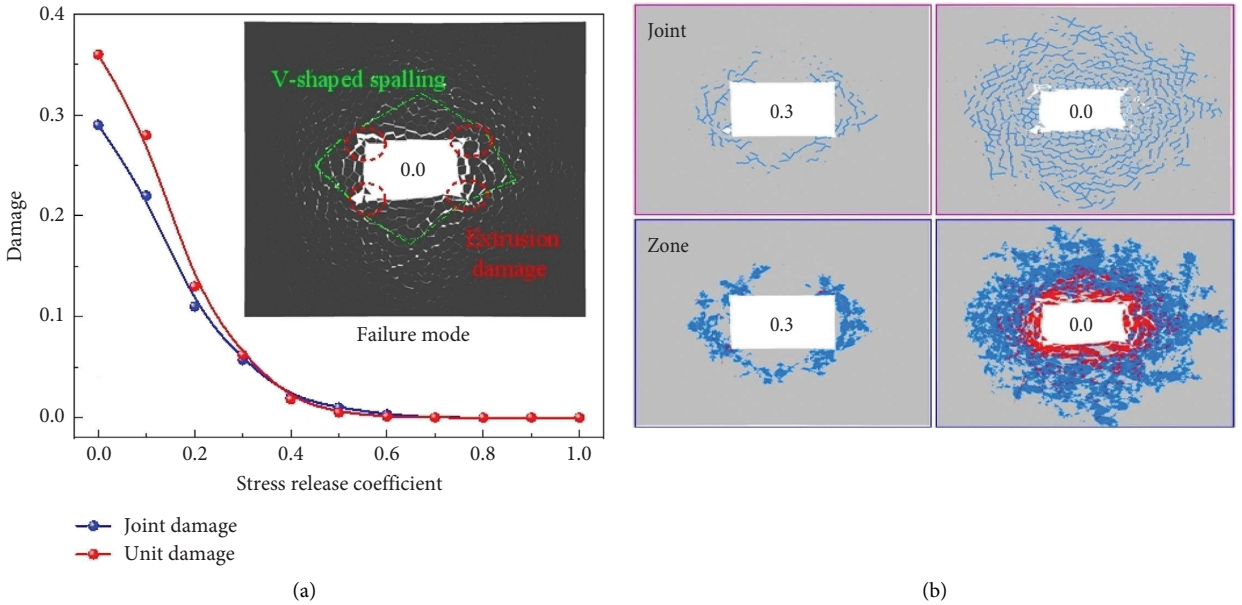

Figure 7: Damage and fracturing characteristics of the surrounding: (a) damage evolution of surrounding rock and (b) distribution characteristics of the plastic zone.

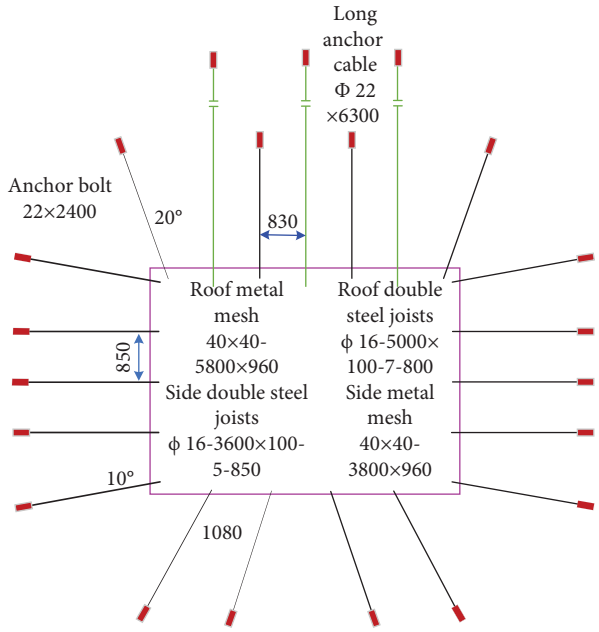

Figure 8: Parameters of roadway support.

appear on the roof. Subsequently, they grew wider and became more widespread, in line with serious roof subsidence during the 6th–15th days.

The anchor bolt and cable experienced a significant increase in load at the beginning of roadway excavation and began to stabilize on the 15th day. In descending order, the magnitudes of load are as follows: the roof anchor cable (190 kN), the roof anchor bolt (96 kN), the left side anchor bolt (78 kN), and the right side anchor bolt (75 kN). Such an order is attributed to the fact that the ground stress was vertical. The anchor bolt and cable had not yet reached their yield limits, indicating that they were in a good stress state with abundant factors. Hence, they could withstand more dynamic loads. In conclusion, with these support parameters, the roadway boasts strong integrity, small surrounding rock deformation, coordinated load on support objects, and high efficiency of multiple support measures. These factors can guarantee a long lifespan of the roadway.

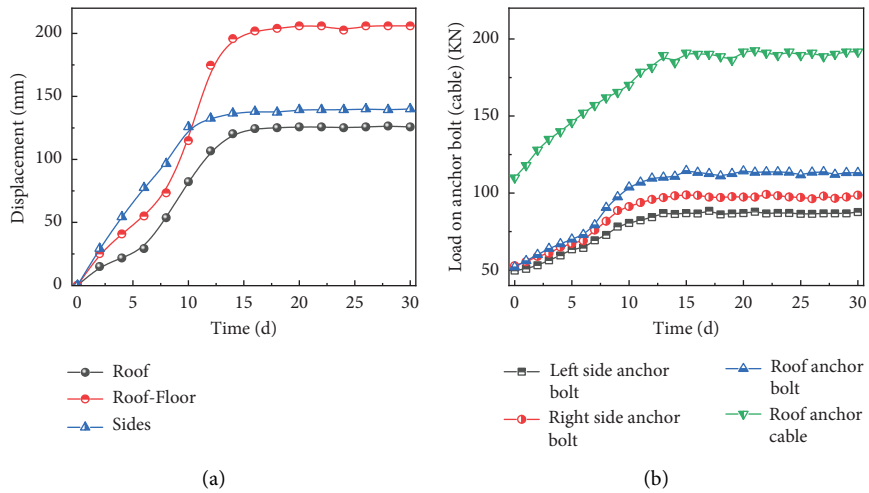

Figure 9: Results of on-site monitoring: (a) deformation of roadway surrounding rock and (b) load on anchor bolt (cable).

5. Conclusions

In this work, the microstructure, macromechanical properties, grade classification, and damage characteristics of the surrounding rock under different stress release coefficients are analyzed, and a surrounding rock reinforcement method applicable to a specific deep roadway is proposed. This method has been successfully applied to supporting deep soft rock roadways in the Yuwu coal industry. However, it has not been tested in other mines, so the study lacks breadth. The scope of application of this study lies in support of deep high-stress soft rock roadways with large span characteristics. The following conclusions are drawn.

(1) Mudstone, which is mainly composed of sodium feldspar (22%) and chlorite (47%), has strong plasticity in the compression phase. However, mudstone will aggravate deformation during the mining process and damage the floor when encountering mine water. Sandstone mainly comprises kaolinite (48%) and quartz (22%) and exhibits pronounced elasticity and brittleness. The surrounding rock on the two sides and floor can be classified as Grade V, while that on the roof is Grade II.

(2) The damage process of a deep soft rock roadway was successfully reproduced by the microparameter calibration model. At an over 60% relaxation state, the roadway surrounding rock will become more plastic and undergo increasingly severe displacement and damage. In this case, appropriate support timing is critical for preventing strong load or irreversible relaxation damage. Postpeak tensile fracturing can indirectly characterize the degree of elasticity and brittleness of the sample.

(3) The mechanism of the large deformation in deep soft rock roadways in the Yuwu coal mine is as follows. The high deviatoric stress causes the formation of the deep V-shaped shear zone. The shallow large-scale tensile free-state surrounding rock gives rise to the discontinuity of stresses in the deep and shallow surrounding rock.

(4) An idea of "timely and active + reinforcing the side and strengthening the bottom" is proposed. Under this approach, the overall convergence of surrounding rock was managed within 350 mm. The stabilization time was about 15 d, and the anchor bolt corresponded to a large abundant factor, thus ensuring the long lifespan of roadways.

Data Availability

The data used to support the findings of this study are included in the article.

Conflicts of Interest

The authors declare that they have no conflicts of interest.

Acknowledgments

This research was funded by the National Natural Science Foundation of China (52107152).

References

[1] G. Li, F. Ma, J. Guo, H. Zhao, and G. Liu, "Study on deformation failure mechanism and support technology of deep soft rock roadway," *Engineering Geology*, vol. 264, Article ID 105262, 2020.

[2] H. Xie, M. Gao, R. Zhang, G. Peng, W. Wang, and A. Li, "Study on the mechanical properties and mechanical response of coal mining at 1000 m or deeper," *Rock Mechanics and Rock Engineering*, vol. 52, no. 5, pp. 1475–1490, 2018.

[3] Q. Wang, S. Xu, Z. Xin, M. He, H. Wei, and B. Jiang, "Mechanical properties and field application of constant resistance energy-absorbing anchor cable," *Tunnelling and*

Underground Space Technology, vol. 125, Article ID 104526, 2022.

[4] D. Ren, X. Wang, Z. Kou et al., "Feasibility evaluation of CO2 EOR and storage in tight oil reservoirs: a demonstration project in the Ordos Basin," *Fuel*, vol. 331, Article ID 125652, 2022.

[5] S. Tang, J. Li, S. Ding, and L. Zhang, "The influence of water-stress loading sequences on the creep behavior of granite," *Bulletin of Engineering Geology and the Environment*, vol. 81, no. 11, p. 482, 2022.

[6] X. Liang, S. Tang, C. A. Tang, L. Hu, and F. Chen, "Influence of water on the mechanical properties and failure behaviors of sandstone under triaxial compression," *Rock Mechanics and Rock Engineering*, vol. 2022, pp. 1–32, 2022.

[7] S. Xie, Y. Wu, D. Chen, R. Liu, X. Han, and Q. Ye, "Failure analysis and control technology of intersections of large-scale variable cross-section roadways in deep soft rock," *International Journal of Coal Science & Technology*, vol. 9, no. 1, p. 19, 2022.

[8] W. Jing, S. Liu, R. Yang, L. Jing, and W. Xue, "Mechanism of aging deformation zoning of surrounding rock in deep high stress soft rock roadway based on rock creep characteristics," *Journal of Applied Geophysics*, vol. 202, Article ID 104632, 2022.

[9] H. Wang, C. Jiang, P. Zheng, W. Zhao, and N. Li, "A combined supporting system based on filled-wall method for semi coal-rock roadways with large deformations," *Tunnelling and Underground Space Technology*, vol. 99, Article ID 103382, 2020.

[10] Q. Liu and L. Sun, "Simulation of coupled hydro-mechanical interactions during grouting process in fractured media based on the combined finite-discrete element method," *Tunnelling and Underground Space Technology*, vol. 84, pp. 472–486, 2019.

[11] Q. Wang, Z. Jiang, B. Jiang, H. Gao, Y. Huang, and P. Zhang, "Research on an automatic roadway formation method in deep mining areas by roof cutting with high-strength bolt-grouting," *International Journal of Rock Mechanics and Mining Sciences*, vol. 128, Article ID 104264, 2020.

[12] X. Xu, H. Jing, Z. Zhao, Q. Yin, J. Li, and H. Li, "Physical model experiment research on evolution process of water inrush hazard in a deep-buried tunnel containing the filling fault," *Environmental Earth Sciences*, vol. 81, no. 20, p. 488, 2022.

[13] G. Li, F. Ma, G. Liu, H. Zhao, and J. Guo, "A strain-softening constitutive model of Heterogeneous rock mass considering Statistical damage and its application in numerical modeling of deep roadways," *Sustainability*, vol. 11, no. 8, p. 2399, 2019.

[14] M. Wang, N. Zhang, J. Li, L. Ma, and P. Fan, "Computational method of large deformation and its application in deep mining tunnel," *Tunnelling and Underground Space Technology*, vol. 50, pp. 47–53, 2015.

[15] K. Yi, H. Kang, W. Ju, Y. Liu, and Z. Lu, "Synergistic effect of strain softening and dilatancy in deep tunnel analysis," *Tunnelling and Underground Space Technology*, vol. 97, Article ID 103280, 2020.

[16] Y. Kang, Q. Liu, G. Gong, and H. Wang, "Application of a combined support system to the weak floor reinforcement in deep underground coal mine," *International Journal of Rock Mechanics and Mining Sciences*, vol. 71, pp. 143–150, 2014.

[17] W. Yu, K. Li, and Z. Zhou, "Deformation mechanism and control technology of surrounding rock in the deep-buried large-span chamber," *Geofluids*, vol. 2020, pp. 1–22, 2020.

[18] X. Guo, Z. Zhao, X. Gao, X. Wu, and N. Ma, "Analytical solutions for characteristic radii of circular roadway surrounding rock plastic zone and their application," *International Journal of Mining Science and Technology*, vol. 29, no. 2, pp. 263–272, 2019.

[19] S.-Q. Yang, M. Chen, H.-W. Jing, K.-F. Chen, and B. Meng, "A case study on large deformation failure mechanism of deep soft rock roadway in Xin'An coal mine, China," *Engineering Geology*, vol. 217, pp. 89–101, 2017.

[20] C. Zhu, Y. Yuan, W. Wang, Z. Chen, S. Wang, and H. Zhong, "Research on the "three shells" cooperative support technology of large-section chambers in deep mines," *International Journal of Mining Science and Technology*, vol. 31, no. 4, pp. 665–680, 2021.

[21] S.-C. Li, H.-T. Wang, Q. Wang et al., "Failure mechanism of bolting support and high-strength bolt-grouting technology for deep and soft surrounding rock with high stress," *Journal of Central South University*, vol. 23, no. 2, pp. 440–448, 2016.

[22] Z. Zhao, Y. Tan, S. Chen, Q. Ma, and X. Gao, "Theoretical analyses of stress field in surrounding rocks of weakly consolidated tunnel in a high-humidity deep environment," *International Journal of Rock Mechanics and Mining Sciences*, vol. 122, Article ID 104064, 2019.

[23] Q. Zhan, X. Zheng, J. Du, and T. Xiao, "Coupling instability mechanism and joint control technology of soft-rock roadway with a buried depth of 1336 m," *Rock Mechanics and Rock Engineering*, vol. 53, no. 5, pp. 2233–2248, 2019.

[24] S. Jia, J. Yang, M. Gao, L. Jia, C. Wen, and G. Wu, "Experimental and numerical analysis of deformation and failure behaviour for deep roadways in soft rocks," *Bulletin of Engineering Geology and the Environment*, vol. 81, no. 11, p. 466, 2022.

[25] Q. Zhan, N. Muhammad Shahani, X. Zheng, Z. Xue, and Y. He, "Instability mechanism and coupling support technology of full section strong convergence roadway with a depth of 1350 m," *Engineering Failure Analysis*, vol. 139, Article ID 106374, 2022.

[26] Q. Zhu, T. Li, Y. Du et al., "Failure and stability analysis of deep soft rock roadways based on true triaxial geomechanical model tests," *Engineering Failure Analysis*, vol. 137, Article ID 106255, 2022.

[27] W. Yuan, K. Hong, R. Liu, L. Ji, L. Meng, and X. Chen, "Numerical simulation of coupling support for high-stress fractured soft rock roadway in deep mine," *Advances in Civil Engineering*, vol. 2022, Article ID 7221168, 10 pages, 2022.

[28] X. Yang, E. Wang, Y. Wang, Y. Gao, and P. Wang, "A study of the large deformation mechanism and control Techniques for deep soft rock roadways," *Sustainability*, vol. 10, no. 4, p. 1100, 2018.

[29] C. Zhao, Y. Li, G. Liu, and X. Meng, "Mechanism analysis and control technology of surrounding rock failure in deep soft rock roadway," *Engineering Failure Analysis*, vol. 115, Article ID 104611, 2020.

[30] Y. Wang, C. Zhu, M. He, X. Wang, and H. Le, "Macro-meso dynamic fracture behaviors of Xinjiang marble exposed to freeze thaw and frequent impact disturbance loads: a lab-scale testing," *Geomechanics and Geophysics for Geo-Energy and Geo-Resources*, vol. 8, no. 5, p. 154, 2022.

[31] Q. Wang, B. Jiang, S. Xu et al., "Roof-cutting and energy-absorbing method for dynamic disaster control in deep coal mine," *International Journal of Rock Mechanics and Mining Sciences*, vol. 158, Article ID 105186, 2022.

[32] Q.-L. Yao, Q. Xu, J.-F. Liu, L. Zhu, D.-W. Li, and C.-J. Tang, "Post-mining failure characteristics of rock surrounding coal

seam roadway and evaluation of rock integrity: a case study," *Bulletin of Engineering Geology and the Environment*, vol. 80, no. 2, pp. 1653–1669, 2020.

[33] F. Gao, D. Stead, and D. Elmo, "Numerical simulation of microstructure of brittle rock using a grain-breakable distinct element grain-based model," *Computers and Geotechnics*, vol. 78, pp. 203–217, 2016.

[34] X. Li, Q. Li, Y. Hu et al., "Study on three-Dimensional dynamic stability of Open-Pit high Slope under Blasting Vibration," *Lithosphere*, vol. 2021, no. 4, Article ID 6426550, 2021.